A comparison of three uncertainty calculi for building sonar-based occupancy grids

Miguel Ribo [a],[*], Axel Pinz [b]

[a] *VRVis Competence Center for Virtual Reality and Visualization, Vienna, Austria*
[b] *Institute of Electrical Measurement and Measurement Signal Processing, Graz University of Technology, Graz, Austria*

Abstract

In this paper, we describe and compare three different uncertainty calculi techniques to build occupancy grids of an unknown environment using sensory information provided by a ring of ultrasonic range-finders. These techniques are based on Bayesian theory, Dempster–Shafer theory of evidence, and fuzzy set theory. Several sensor models are presented to handle uncertainty according to the selected building procedure. Experimental examples of occupancy grids, built from real data recorded by two different mobile robots in office-like environment, are presented to perform a comparison among the proposed calculi techniques. Probabilistic and evidence theoretic methods are more accurate in structured environments, while in cases of multiple reflections only the possibilistic approach provides correct results. © 2001 Published by Elsevier Science B.V.

Keywords: Mobile robots; Sonar-based occupancy grids; Bayesian theory; Dempster–Shafer theory of evidence; Fuzzy set theory

1. Introduction

The performance of an autonomous mobile robot for navigating in an unknown environment depends strongly on the accuracy of its perception capabilities. The system needs to gather a large amount of sensory information and to integrate it into a proper representation of the environment. The traditional paradigm to recover spatial information is based on the use of a two-dimensional tessellation called *occupancy grid* (OG): it was first introduced by Moravec and Elfes [1], and is widely used as mapping support in mobile robot navigation. In principle, OGs store qualitative information about which areas of the robot's surroundings are (completely) empty, and which areas are (even partially) occupied by obstacles. Besides, no other characterization of the environment is of interest.

Ultrasonic range-finders are common in mobile robot navigation due to their simplicity of operation and high working speed. These sensors provide relative distances between them and surrounding obstacles located within their radiation cone. The time elapsed between the transmission of a wave and the reception of its echo allows the computation of a range reading r. This means that an obstacle may be located *somewhere* on the arc of radius r within the sensor beam. However, these devices are prone to several measuring errors due to various phenomena (e.g., multiple reflections, wide radiation cone, low angular resolution). As a consequence, the sensing process is affected by a large amount of uncertainty which needs to be modeled efficiently (i.e., with respect to the selected methodology), in order to handle uncertainty during the occupancy grid building process.

---

* Corresponding author.
E-mail addresses: ribo@vrvis.at (M. Ribo), pinz@emt.tu-graz.ac.at (A. Pinz).
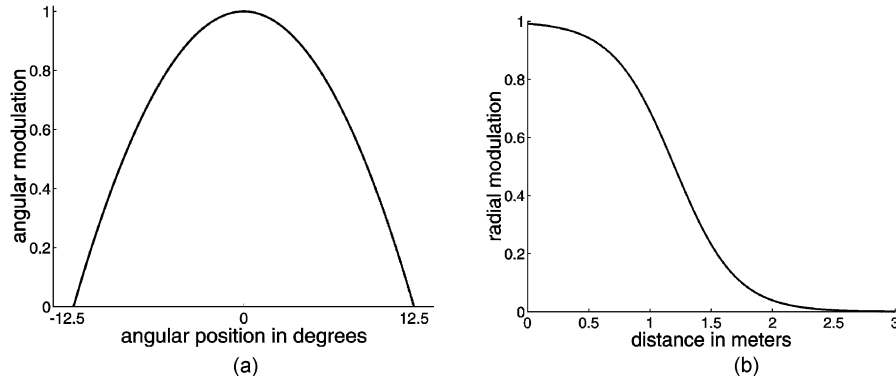
Fig. 1. Behavior of the sonar sensors: (a) the angular modulation function $\Gamma(\theta)$, and (b) the radial modulation function $\Delta(\rho)$ with $\rho_v = 1.2$ m.

In this paper, we present and compare three different approaches to build sonar-based OGs. These approaches are based on Bayesian theory [2,3], Dempster–Shafer theory of evidence [4,5], and fuzzy set theory [6,7]. As testbed, we have used ultrasonic range information provided by two different mobile robots (the Robuter III from RobotSoft and the B21 from Real World Interface) navigating into two different office-like environments. Each robot is equipped with a ring of 24 Polaroid ultrasonic range transducers with radiation cones of $25°$ width.

2. Uncertainty approaches to OG-building

Let us consider an environment universe U discretized into a bitmap structure of $m \times n$ cells C_{ij}, each of size $\delta \times \delta$. Formally, the set U can be written as

$$U = \{C_{ij} | i \in [1..m], j \in [1..n]\}. \qquad (1)$$

A set of range readings $R = \{r_1, \ldots, r_p\}$ collected at known locations $L = \{l_1, \ldots, l_q\}$ is available. In principle, the purpose of the sonar-based OG building system will be to integrate, along the path $[l_1 l_2 \ldots l_q]$, all data in R. As a result, our OG may represent the surroundings of the robot in which each cell C_{ij} carries a confidence rate of whether it is *empty* (E) or *occupied* (O) by an object in the environment. These rates are obtained by applying sensor models (cf. Sections 2.1–2.3), that quantify the uncertainty in the range data, over the prior estimate of the OG.

For modeling the general behavior of the sonar sensors in angular and range resolution, independently of the selected approach, we introduce the following two functions (see [6] for more detailed information)

$$\Gamma(\theta) = \begin{cases} 1 - 21\left(\dfrac{\theta\pi}{180}\right)^2, & 0 \leqslant |\theta| \leqslant 12.5°, \\ 0, & |\theta| > 12.5°, \end{cases} \qquad (2)$$

$$\Delta(\rho) = 1 - \frac{1 + \tanh(2(\rho - \rho_v))}{2}, \qquad (3)$$

where θ is the angular distance to the beam axis, ρ the radial distance to the sensor, and ρ_v a predefined distance from the sensor where a smooth transition occurs from certainty to uncertainty. The function Γ, shown in Fig. 1(a), reflects the fact that the intensity of the waves decreases to zero at the borders of the radiation cone: the degree of confidence is assumed to be higher for points close to the beam axis.[1] The function Δ, shown in Fig. 1(b), quantifies the degree of confidence for the detection of an obstacle as the distance from the sensor increases.

2.1. Probabilistic approach

The Bayesian method rules the greatest part of the work related to the probabilistic sensor fusion in building OGs. This attraction stems from the property of the

---

[1] In fact, Γ is a second-order polynomial function that approximates the beam pattern of the transmitter which is a Bessel function.

Bayes' updating rule which facilitates recursive and incremental schemes [8]. However, in order to avoid huge calculation processes one must assume that the cell states are *independent*. Indeed, for an occupancy grid with $m \times n$ cells, each cell with two possible states, it would be necessary to specify 2^{mn} conditional probabilities.

The goal of the proposed approach is to determine the *probability* of each cell to be occupied [2,3], the state variable $s(C_{ij})$ associated to the cell C_{ij} is defined as an independent discrete random variable with two states (E and O). Besides, for all C_{ij} in U the constraint $P[s(C_{ij}) = E] + P[s(C_{ij}) = O] = 1$ is applied. This means that each cell has an associated probability mass function (i.e., $P[s(C_{ij}) = O|r] \in [0, 1]$) which is estimated by the sensor interpretation and integration process.

The sensor model used here to interpret the uncertainty in range data is denoted as follows

$$p[r|s(C_{ij}) = O]$$
$$= p_1[r|s(\theta, \rho) = O] + p_2(\theta, \rho), \qquad (4)$$

$$p_1[r|s(\rho, \theta) = O]$$
$$= \begin{cases} (1 - \lambda)(0.5 - p_E), \\ \qquad 0 \leqslant \rho < r - 2\delta r, \\ (0.5 - p_E)\left(1 - \lambda\left(\dfrac{(r + \delta r) - (\rho - \delta r)}{\delta r}\right)^2\right), \\ \qquad r - 2\delta r \leqslant \rho < r - \delta r, \\ \lambda(p_O - 0.5)\left(1 - \left(\dfrac{r - \rho}{\delta r}\right)\right)^2, \\ \qquad r - \delta r \leqslant \rho < r + \delta r, \\ 0.5, \qquad \rho \geqslant r + \delta r, \end{cases} \qquad (5)$$

$$p_2(\rho, \theta) = \begin{cases} p_E, & 0 \leqslant \rho < r - \delta r, \\ 0.5, & \rho \geqslant r - \delta r, \end{cases} \qquad (6)$$

where p_E and p_O are the minimum and maximum values reached by the function p_S such that $p_E + p_O = 1$, r is a given range reading, $2\delta r$ is the width of the area considered 'proximal' to the arc of radius r, ρ is the distance from the sensor to C_{ij}, θ is the angular distance between the beam axis and C_{ij}, and $\lambda = \Delta(\theta) \cdot \Gamma(\rho)$. The 3D profile of Eq. (4) is depicted in Fig. 2.
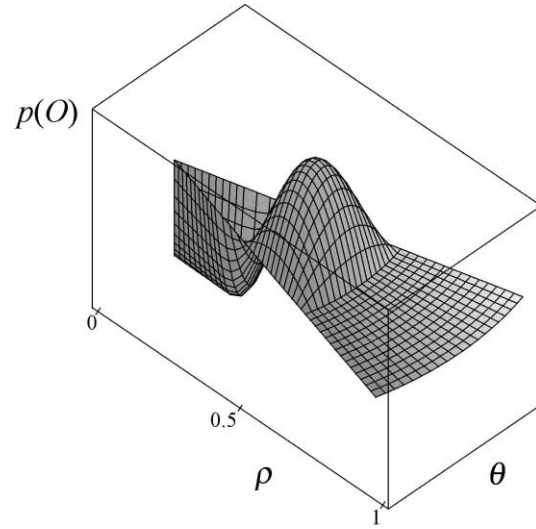

Fig. 2. 3D profile of the sensor model used to interpret range data in the probabilistic approach with $r = 0.5$ m.

Furthermore, the building procedure of a probabilistic occupancy grid using the sensor model (4) can be expressed by the updating process as

$$P[s(C_{ij}) = O|r]$$
$$= \frac{p[r|s(C_{ij}) = O]P[s(C_{ij}) = O]}{\displaystyle\sum_{X \in \{E, O\}} p[r|s(C_{ij}) = X]P[s(C_{ij}) = X]}, \qquad (7)$$

where r is the measured range by the sonar sensor, $P[s(C_{ij}) = X]$ ($X \in \{E, O\}$) is the prior estimate of the cell state, and $p[r|s(C_{ij}) = X]$ ($X \in \{E, O\}$) is determined from the sensor model (we note that $p[r|s(C_{ij}) = E] = 1 - p[r|s(C_{ij}) = O]$). At the beginning the OG is set up with $P[s(C_{ij}) = O] = P[s(C_{ij}) = E] = 0.5$, $\forall C_{ij} \in U$ (i.e., the state of the occupancy grid is set to 'unknown').

2.2. Evidence theoretic approach

The implemented approach finds its formulation through the use of Dempster–Shafer theory of evidence [4,5]. In this case, the goal of the OGs' building procedure is to determine the *support* for the propositions E and O. Thus, we define the *set of discernment* by $\Omega = \{E, O\}$, and the *set of propositions* by $\Lambda = 2^\Omega = \{\emptyset, E, O, \{E, O\}\}$. The state of each cell

C_{ij} is defined by assigning *mass functions* m_{ij} to each label in Λ, such that (assuming $m_{ij}(\emptyset) = 0$)

$$\forall C_{ij} \in U, \quad m_{ij}(E) + m_{ij}(O) + m_{ij}(\{E, O\}) = 1. \quad (8)$$

In this approach, two different sensor models are involved, one for the proposition E and the other for the proposition O, to interpret uncertainty in range data. Their formulation can be done as follows:

$$m_{ij}^{S(r)}(E) = \Gamma(\theta) \cdot \Delta(\rho) \cdot f_E(\rho, r) \quad \text{and}$$
$$m_{ij}^{S(r)}(O) = \Gamma(\theta) \cdot \Delta(\rho) \cdot f_O(\rho, r), \quad (9)$$

$$f_E(\rho, r) = \begin{cases} k_E, & 0 \leqslant \rho < r - \delta r, \\ k_E \left(\dfrac{r - \rho}{\delta r} \right)^2, & r - \delta r \leqslant \rho < r, \\ 0, & \rho \geqslant r, \end{cases} \quad (10)$$

$$f_O(\rho, r)$$
$$= \begin{cases} 0, & 0 \leqslant \rho < r - \delta r, \\ k_O \left(1 - \left(\dfrac{r - \rho}{\delta r} \right)^2 \right), & r - \delta r \leqslant \rho < r + \delta r, \\ 0, & \rho \geqslant r + \delta r, \end{cases} \quad (11)$$

where k_E and k_O are the maximum values, such that $k_E + k_O \leqslant 1$, reached by the functions f_E and f_O,

respectively. r is a given range reading, $2\delta r$ is the width of the area considered 'proximal' to the arc of radius r, ρ is the distance from the sensor to C_{ij}, and θ is the angular distance between the beam axis and C_{ij}. The 3D profiles of Eq. (9) are depicted in Fig. 3.

Furthermore, the building procedure of an evidential OG using the sensor models (9) can be expressed by the updating processes as

$$\forall A \in \Omega,$$
$$m_{ij}^{M} \oplus m_{ij}^{S(r)}(A)$$
$$= \frac{\displaystyle\sum_{\forall B, C \in \Lambda | B \cap C = A} m_{ij}^{M}(B) m_{ij}^{S(r)}(C)}{1 - \displaystyle\sum_{\forall B, C \in \Lambda | B \cap C = \emptyset} m_{ij}^{M}(B) m_{ij}^{S(r)}(C)}, \quad (12)$$

where m_{ij}^{M} are the mass functions of the stored OGs. At the beginning the OGs are set up with $m_{ij}^{M}(E) = m_{ij}^{M}(O) = 0$ and $m_{ij}^{M}(\{E, O\}) = 1, \forall C_{ij} \in U$ (i.e., representing the total ignorance about the state of each cell).

2.3. Possibilistic approach

The basic idea [6,7] is that the empty and the occupied areas are defined as two *fuzzy sets*. We denote them by $\mathcal{E}$ and $\mathcal{O}$, and their membership functions
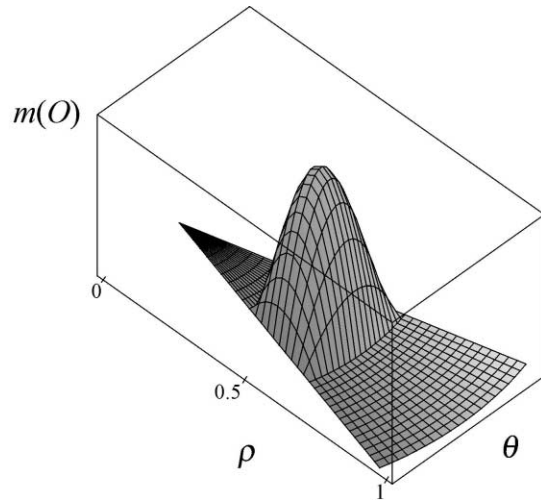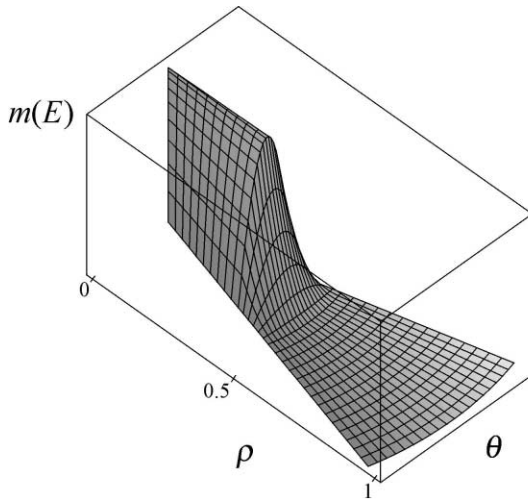

Fig. 3. 3D profiles of the sensor models used to interpret range data in the evidence theoretic and fuzzy logic approaches with $r = 0.5\,\text{m}$ (models for empty cells (left) and for occupied cells (right), adapted from [6]).

by $\mu_{\mathcal{E}}$ and $\mu_{\mathcal{O}}$, respectively. Besides, we assume that these two sets are no longer complementary: for a given cell, partial membership to $\mathcal{E}$ and $\mathcal{O}$ is possible. This allows to identify areas where sonar observations have provided conflicting or insufficient information, in order to build conservative OGs of the environment. As a result, the goal of the building process is to quantify the possibility of each cell to belong to an obstacle.

Therefore, as in Section 2.2, two different sensor models are needed. We denote them as follows:

$$\mu_{\mathcal{E}}^{S(r)}(C_{ij}) = \Gamma(\theta) \cdot \Delta(\rho) \cdot f_E(\rho, r) \quad \text{and}$$
$$\mu_{\mathcal{O}}^{S(r)}(C_{ij}) = \Gamma(\theta) \cdot \Delta(\rho) \cdot f_O(\rho, r), \qquad (13)$$

where f_E and f_O are defined such that $k_E \leqslant 1$ and $k_O \leqslant 1$ (cf. Eqs. (10) and (11)). The 3D profiles of Eq. (13) are depicted in Fig. 3.

Furthermore, the building procedure of a fuzzy OG using the sensor models (13), can be expressed by the updating processes as

$$\forall \mathcal{X} \in \{\mathcal{E}, \mathcal{O}\},$$
$$\mu_{\mathcal{X}}^{M}(C_{ij}) = \mu_{\mathcal{X}}^{M}(C_{ij}) + \mu_{\mathcal{X}}^{S(r)}(C_{ij})$$
$$\qquad - \mu_{\mathcal{X}}^{M}(C_{ij}) \cdot \mu_{\mathcal{X}}^{S(r)}(C_{ij}), \qquad (14)$$

where $\mu_{\mathcal{X}}^{M}$ ($\forall \mathcal{X} \in \{\mathcal{E}, \mathcal{O}\}$) are the membership functions of the stored OGs. At the beginning the OGs are set up with $\mu_{\mathcal{E}}^{M}(C_{ij}) = \mu_{\mathcal{O}}^{M}(C_{ij}) = 0, \forall C_{ij} \in U$ (i.e., representing the total ignorance about the state of each cell).

Finally, we compute the set of *ambiguous* cells $\mathcal{A}$ whose elements are both 'empty' and 'occupied', and the set of *indeterminate* cells $\mathcal{I}$ whose elements are neither 'empty' nor 'occupied'. Then, the set $\mathcal{S}$ of the safe cells [2] is calculated as follows

$$\mathcal{S} = \mathcal{E}^2 \cap \bar{\mathcal{O}} \cap \bar{\mathcal{A}} \cap \bar{\mathcal{I}}$$
$$\text{with } \mathcal{A} = \mathcal{E} \cap \mathcal{O} \text{ and } \mathcal{I} = \bar{\mathcal{E}} \cap \bar{\mathcal{O}}, \qquad (15)$$

where we use the *complement* operator $\bar{\mu}_{\mathcal{X}}(C_{ij}) = 1 - \mu_{\mathcal{X}}(C_{ij})$, and the *algebraic product* $\mu_{\mathcal{X} \cap \mathcal{Y}}(C_{ij}) = \mu_{\mathcal{X}}(C_{ij}) \cdot \mu_{\mathcal{Y}}(C_{ij}), \forall C_{ij} \in U$. We note the conservative character of $\mathcal{S}$ by 'discarding' *ambiguous* and *indeterminate* cells from the building procedure.

---

[2] $\mathcal{S}$ characterizes a refined fuzzy OG (see for more details [6,9]).

3. Experimental results

The three presented approaches were implemented in C on a Silicon Graphics Indy workstation running under UNIX, and were used to build OGs of two different office-like environments (Fig. 4(a) and (e)). The experimental real range data were gathered by two robots throughout their whole trajectory.

As far as localization problems are concerned in our experimental results, we use the ground truth provided by the odometric system of the mobile robots. In this way, we rely on odometry measurements to estimate the position of the robots corresponding to each range reading. Indeed, the estimation errors of the robot's position along the whole trajectories are less than the grid sizes of the OGs (i.e., 10 cm for the first environment, and 5 cm for the second one).

The first environment (7.3 m × 4.5 m) is depicted in Fig. 4(a). It involves three obstacles (a cardboard box in the middle of the room, a power supply box in the middle of the left wall, and an other robot in the top left-hand corner) where the robot moves around to record the data returned by the sensory devices. The universal set U was discretized into a matrix of 54×110 cells of size $\delta = 10$ cm. The trajectory of the robot is shown superimposed ('+' marks the starting point) and represents a set of 141 measurement locations (at each location, the sonar ring of the robot provides 24 range readings then the whole data set is about 3384 range values): we denote this set as 'data-set-1'.

The second environment (6 m × 2.2 m) is depicted in Fig. 4(e). The room is characterized by a set of book shelves with rough surfaces which may cause a smooth sonar echo (on the right-hand side), and a wall with two open doors with a flat surface which may induce multiple reflections (on the left-hand side). The set U was discretized into a matrix of 85×170 cells of size $\delta = 5$ cm. The trajectory of the robot represents a set of 71 measurement locations (the whole data set is about 1704 range values): we denoted this set as 'data-set-2'.

We have used the following set of parameter values: $\rho_v = 1.2$ m, $\delta r = 0.15$ m, $p_O = 0.6$ for the probabilistic approach (see Section 2.1), $k_E = 0.25$ and $k_O = 0.45$ for the evidence theoretic approach (see Section 2.2), $k_E = 0.45$ and $k_O = 0.65$ for the possibilistic approach (see Section 2.3).
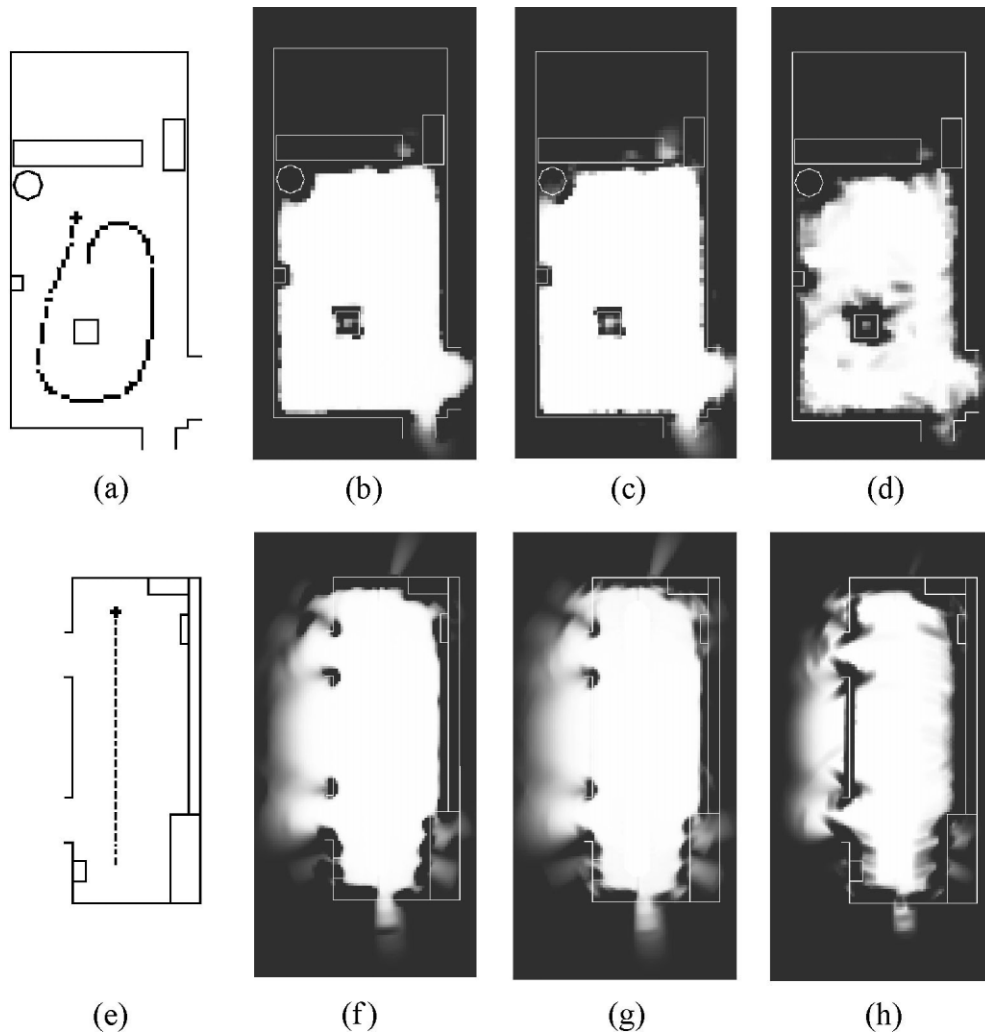
Fig. 4. (a) and (e) The two experimental environments, and the resulting OGs using (b) and (f) the probabilistic, (c) and (g) the evidence theoretic, and (d) and (h) the possibilistic approaches. The lighter areas correspond to the 'safe' cells. The '+' shows the starting point of the whole trajectory.

After an integration of all the data along the trajectory of the robots, the resulting OGs are shown in Fig. 4 as gray-level density plots of U, where lighter areas represent the 'safe' cells while darker areas represent the 'unsafe' cells.

4. Comparisons and conclusion

In a structured environment (Fig. 4(a)), in the absence of multiple reflections (they may occur for large

angles of incidence between sonar echoes and surfaces that reflect them), all the three methods provide suitable OGs (Fig. 4(b)–(d)). We can see the satisfactory concordance of the three OGs with the profile of the room. However, a preference can be granted to the probabilistic and evidence theoretic approaches thanks to their better definition of boundaries (see for instance Fig. 5(b) and (d), and also Fig. 4(f) and (h) on the right side). We achieve a maximum distance no greater than 3 cells between the contour of the two OGs and the profile of the room. On the other hand, the

conservative character of the fuzzy OG enlarges the contour of the detected boundaries (Fig. 5(f) on top) and produces some undesirable artefacts (Fig. 5(f) on bottom). The maximum distance between the contour of the OG and the profile of the room is about 5 cells. We can remark that such a behavior can induce difficulties to a trajectory planner for providing accurate navigation paths between obstacles.

In presence of multiple reflections (Fig. 4(e)–(h)), only the possibilistic approach provides the correct results: the building process is more robust towards outliers. The building algorithm has correctly found the boundary of the flat wall on the left side of the environment (Fig. 4(h)). After a processing of 15 range readings, the three proposed approaches do not detect the wall located after the door. Referring to Fig. 5(a), (c) and (e) on the left column, we can see light gray areas extending beyond the boundary of the wall. In this case, the set of sensors S_1 located on the front-right side of the platform (the superimposed continuous line shows the main direction of S_1) has a large angle of incidence with respect to the surface of the wall. This may induce multiple reflections and mislead range measurements: the readings provided by S_1 are longer than the "real" values. After an integration of 10 additional range readings, the resulting OGs are shown in Fig. 5(a), (c) and (e) on the right column. In this case, the set of sensors S_2 located on the right side
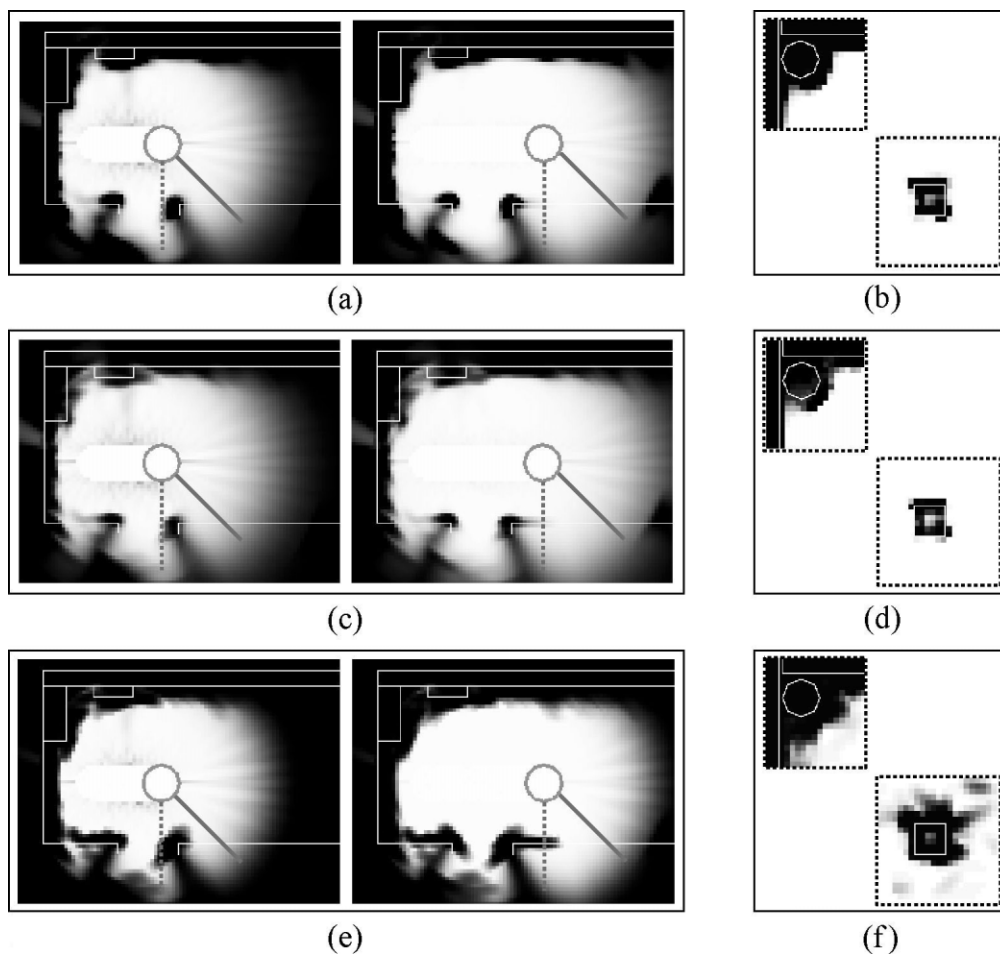

Fig. 5. Details of OGs building processes ((a), (c) and (e)) and delineations of obstacles ((b), (d) and (f)): (a) and (b) probabilistic, (c) and (d) evidence theoretic, (e) and (f) possibilistic.

of the platform may provide reliable measurements. Indeed, the main direction of S_2 (the superimposed dashed line) is perpendicular to the surface of the wall. However, for the probabilistic and evidence theoretic approaches (Fig. 5(a) and (c)) the range readings provided by S_2 do not infer the detection of the boundary of the wall. On the contrary, the conservative behavior of the possibilistic approach (Fig. 5(e)) advantageously uses the data of S_2 and produces the correct detection of the wall.

The building algorithm of the probabilistic approach is the fastest and has minimum memory consumption. The processing times for the evidence theoretic and possibilistic approaches are approximately 1.5 times higher than for the probabilistic approach. Concerning the stored OGs, the possibilistic approach is the one with the highest memory requirement. This could be a drawback and might require compact representations, e.g., quad trees to store the processed OGs.

To sum up, within a general framework of navigation in mobile robotics, the possibilistic approach may produce the most suitable OGs thanks to its robustness with respect to outliers. The probabilistic and the evidence theoretic approaches produce good results in certain cases, but their performances with respect to outliers are very poor. However, a possible criticism to the possibilistic approach is the conservative behavior of its building process. It can infer the loss of information in certain parts of the explored environment (see open doors in Fig. 4(h)) and induce the emergence of some artifacts in the OG (Fig. 5(f) on the bottom). In this way, we can achieve less accuracy in the detected boundaries, in the case of narrow areas (e.g., open doors), and surfaces causing the loss of some information (e.g., the book shelves on the right side of the environment, Fig. 4(f)–(h)). Nevertheless, as we show in [9], by fusing both sonar and visual [3] fuzzy OGs we can improve the accuracy of the detected boundaries and recover information missing from sonar data alone.

Acknowledgements

References

[1] H.P. Moravec, A. Elfes, High resolution maps from wide angle sonar, in: Proceedings of the IEEE International Conference on Robotics and Automation, St. Louis, MO, March 1985, pp. 116–121.

[2] A. Elfes, Multi-source spatial data fusion using Bayesian reasoning, in: M.A. Abidi, R.C. Gonzales (Eds.), Data Fusion in Robotics and Machine Intelligence, Academic Press, New York, 1992 (Chapter 3).

[3] L. Matthies, A. Elfes, Integration of sonar and stereo range data using a grid-based representation, in: Proceedings of the IEEE International Conference on Robotics and Automation, Philadelphia, PA, April 1988, pp. 727–733.

[4] F. Gambino, G. Ulivi, M. Vendittelli, The transferable belief model in ultrasonic map building, in: Proceedings of the Sixth IEEE International Conference on Fuzzy Systems, Barcelona, Spain, July 1997, pp. 601–608.

[5] D. Pagac, E.M. Nebot, H. Durrant-Whyte, An evidential approach to map-building for autonomous vehicles, IEEE Transaction on Robotics and Automation 14 (4) (1998) 623–629.

[6] G. Oriolo, G. Ulivi, M. Vendittelli, Fuzzy maps: A new tool for mobile robot perception and planning, Journal of Robotic Systems 14 (3) (1997) 179–197.

[7] G. Oriolo, G. Ulivi, M. Vendittelli, Real-time map building and navigation for autonomous robots in unknown environments, IEEE Transactions on Systems, Man, and Cybernetics 28 (3) (1998) 318-333.

[8] J. Pearl, Probabilistic Reasoning in Intelligent Systems: Networks of Plausible Inference, Morgan Kaufmann, Los Altos, CA, 1988.

[9] M. Ribo, A. Pinz, A fuzzy framework for multi-sensor fusion in mobile robot navigation, in: Proceedings of the EuroFusion'98, Data Fusion Conference, Great Malvern, UK, October 1998, pp. 15–21.

[10] C. Peignot, F. Wawak, F. Matía, E.A. Puente, Integration of heterogeneous world mapping techniques in the navigation system of an autonomous mobile robot, in: Proceedings of the Computer Vision and Mobile Robotics Workshop, Santorini, Greece, September 1998, pp. 54–58.

---

[3] Thanks to a stereo rig fixed on the top of the mobile robot.

Miguel Ribo was born in Carthago, Tunisia, in 1969. He received his D.E.A. diploma in computer vision, image processing and robotics (1996) from the University of Nice-Sophia Antipolis, France and Ph.D. in computer engineering (2000) from Graz University of Technology, Austria. In the 1996–1997 period, he worked as a Research Assistant at the Institute for Systems and Robotics (Lisbon, Portugal) on autonomous robot navigation (European project MAUVE). In the 1997–2000 period, he worked as a Research Assistant at the Institute for Computer Graphics and Vision (Graz, Austria) on vision-based robot navigation and data fusion (European project VIRGO). Since June 2000, he is working as a Senior Researcher at the Research Center for Virtual Reality and Visualization (Vienna, Austria). His research interests include real-time machine vision, autonomous robot navigation, data fusion, spatial representation, and augmented reality.

Axel Pinz was born in Vienna, Austria, in 1958. He received his M.Sc. degree in electrical engineering (1983), Ph.D. in computer science (1988) from Vienna University of Technology, and the Habilitation in Computer Science (1995) from Graz University of Technology, Austria. He has worked in the areas of image processing, pattern recognition, computer vision, and computer graphics over the past 15 years. He has supervised or co-supervised over 50 Master's Thesis and 24 Ph.D. Thesis students in these areas, and published more than 130 scientific papers. Currently he is an Associate Professor at Graz University of Technology, Institute of Electrical Measurement and Measurement Signal Processing. Axel Pinz is a member of IEEE and INNS, and currently he is the Chairman of the AAPR (Austrian Association for Pattern Recognition), the Austrian chapter of the IAPR. His research interests are in the areas of high-level vision, object recognition, and information fusion, as well as real-time vision with applications in robotics, augmented reality, medical image analysis, and remote sensing.